*Inorg. Chem.* **2003**, *42*, 5938–5948

Inorganic Chemistry

Article

# Design of High-Dimensional Copper(II) Malonate Complexes with Exo-Polydentate N-Donor Ligands

**Fernando S. Delgado,[†] Joaquín Sanchiz,[‡] Catalina Ruiz-Pérez,*,[†] Francesc Lloret,[§] and Miguel Julve[§]**

*Laboratorio de Rayos X y Materiales Moleculares, Departamento de Física Fundamental II, Universidad de La Laguna, Avda. Astrofísico Francisco Sánchez s/n, 38206 La Laguna, Tenerife, Spain, Laboratorio de Rayos X y Materiales Moleculares, Departamento de Química Inorgánica, Universidad de La Laguna, Avda. Astrofísico Francisco Sánchez s/n, 38204 La Laguna, Tenerife, Spain, and Departament de Química Inorgànica/Instituto de Ciencia Molecular, Facultat de Química, Universitat de València, 46100 Burjassot, València, Spain*

Received April 21, 2003

Two polymeric malonato-bridged copper(II) complexes of formulas $\{(H_2bpe)[Cu(mal)_2]\}_n \cdot 4nH_2O$ (**1**) and $[Cu_4(mal)_4(bpe)_3]_n \cdot 6nH_2O$ (**2**) [mal = malonate dianion; bpe = 1,2-bis(4-pyridyl)ethylene] have been synthesized and characterized by X-ray diffraction. Complex **1** crystallizes in triclinic space group $P\bar{1}$, $Z = 1$, with unit cell parameters $a = 4.8831(10)$ Å, $b = 9.585(2)$ Å, $c = 11.813(2)$ Å, $\alpha = 77.29(3)°$, $\beta = 82.18(3)°$, and $\gamma = 84.92(3)°$, whereas complex **2** crystallizes in the monoclinic space group $P2_1/n$, $Z = 4$, with unit cell parameters $a = 13.462(3)$ Å, $b = 10.275(5)$ Å, $c = 19.579(4)$ Å, and $\beta = 105.21(3)°$. The structure of **1** consists of anionic malonato-bridged uniform copper(II) chains which are connected through hydrogen bonds involving malonate-oxygen atoms, noncoordinated water molecules, and $H_2bpe^{2+}$ cations. The intrachain copper–copper separation through carboxylate-malonate bridge in the *anti–syn* conformation is 4.8831(10) Å. Complex **2** possesses a three-dimensional structure made up of neutral corrugated malonated-bridged copper(II) layers linked through bis-monodentate bpe molecules. The copper(II) atoms within each layer are bridged by a double $\mu$-oxo and four carboxylato-malonate bridges with copper–copper separations of 3.4095(7) Å (through oxo) and 4.9488(11)–6.5268(13) Å (through carboxylato). The shortest interlayer copper–copper separation across bridging bpe is 13.434(3) Å. Variable-temperature magnetic measurements (2–290 K) show an overall ferromagnetic behavior for both compounds. The magnetic pathway of complex **1** is through a single carboxylate–malonate bridge connecting apical and equatorial positions of adjacent copper(II) atoms, and the value of the magnetic coupling ($J$) for **1** through a numerical expression for a ferromagnetic uniform chain of interacting local doublets is $J = +0.049(1)$ cm$^{-1}$. The values for the magnetic couplings through the main intralayer exchange pathways in **2** which correspond to carboxylate–malonate bridges connecting equatorial–equatorial ($J_1$) and equatorial–apical ($J_2$) coordination sites and to the double $\mu$-oxo bridge linking equatorial–apical ($J_5$) positions have been determined through a simplified model. The three magnetic couplings are weak, two of them being ferromagnetic ($J_1 = +23(1)$ cm$^{-1}$ and $J_2 = +6.5(1)$ cm$^{-1}$) and the other one antiferromagnetic [$zJ' = -1.0(1)$ cm$^{-1}$]. The values of the magnetic couplings in **1** and **2** compare well with those previously reported for similar malonato-bridged copper(II) complexes of different dimensionalities.

## Introduction

The interest in the design of supramolecular coordination networks has permanently increased during the past decade.[1−6] In this respect, the concept of a molecular building block or tecton[5] in the context of supramolecular synthesis[7] afforded a large number of new coordination topologies with different metrics. The control of the network parameters through a careful selection of the metal ion and organic bridging ligands offers new possibilities for developing functional materials with useful properties. Open framework structures promise catalysts with extra productivity that take advantage of the

---

* Corresponding author. E-mail: caruiz@ull.es.

[†] Laboratorio de Rayos X y Materiales Moleculares, Departamento de Física Fundamental II, Universidad de La Laguna.

[‡] Laboratorio de Rayos X y Materiales Moleculares, Departamento de Química Inorgánica, Universidad de La Laguna.

[§] Departament de Química Inorgánica/Instituto de Ciencia Molecular, Facultat de Química, Universitat de València.

(1) Batten, S. R.; Robson, R. *Angew. Chem., Int. Ed.* **1998**, *37*, 1460.
(2) Robson, R. *J. Chem. Soc., Dalton Trans.* **2000**, *21*, 3735.

10.1021/ic034422w CCC: $25.00

crystallinity,[8] selective and/or reversible adsorbents, materials possessing new properties due to incorporation in the tight pores with sides acting as scaffolds,[4] and acentric inclusion compounds that may exhibit useful electrical and optical[9] features. Other interesting aspects of these networks are provided by factors such as their anisotropy or structuration.[10,11]

*exo*-Polydentate N-donor ligands such as 4,4′-bipyridine (4,4′-bpy) and pyrazine (pyz)[4] are suitable examples of the tectons that are currently employed for the rational design of solid state functionality. The metal assembling into predictable multidimensional structures becomes easier having in mind the structural simplicity and well-known coordination modes of these ligands. The control of the metrics of the resulting net arrays and their inherent properties by carefully tuning the tecton structure, donor properties, and mutual spatial alignment of binding sites seems very attractive. In this context, novel perspectives for the design of coordination polymers may be offered by molecules that have the structural simplicity of the described ligands and special properties such as the ability to form coordination polymers both in neutral and anionic forms and to serve as efficient donors of hydrogen bonds for effective control of the counterion position and enclathration of hydrophilic guest species.

In our recent work, increasing attention has been paid to the construction of two- or three-dimensional (2D or 3D) magnetic systems in order to gain a better understanding of the correlation between structure and magnetism.[12−14] A suitable strategy to build a spatial well-spanned framework is to use certain features of potential ligands, such as the conformational flexibility, diversity of binding modes, and ability to form hydrogen bonds. In this regard, malonate (mal) and 1,2-bis(4-pyridyl)ethylene (bpe) can be used as useful connectors to assemble paramagnetic centers into high-dimensional molecular arrangements.

The malonate ligand can form multidimensional compounds owing to its multibinding ability with regard to metal ions.[12−14] Concerning the bpe ligand, it has a broad relevance in the construction of the solid state architectures and crystal engineering[15] due to its conformational flexibility and coordinating and hydrogen bonding abilities.

Hydrogen bonding, which is the important directional interaction responsible for the supramolecular arrangement and the significant factor in crystal engineering,[16] has a drawback in the field of molecular magnetism since hydrogen-bonded systems cannot provide enhanced magnetic interactions to the extent that covalent-bonded systems do. Therefore, the preparation of purely covalent-bonded high-dimensional systems is particularly crucial in the field of molecule-based magnets, and the coupled use of types of bridging ligands seems to be a reasonable synthetic strategy, although examples still remain scarce.[17] In addition, the transformation of noncovalent/covalent systems to high-dimensional covalent systems has not been thoroughly investigated. Thus, we explored these two aspects employing the appropriate combinations of the mal and bpe ligands and the hydrogen bond to prepare new magnetically coupled systems with blended bridges. Here, we report the synthesis, structure, and magnetic properties of a hydrogen- and covalent-bonded 2D polymer $\{(H_2bpe)[Cu(mal)_2]\}_n{\cdot}4nH_2O$ (**1**) and a covalent-bonded 3D network $[Cu_4(mal)_4(bpe)_3]_n{\cdot}6nH_2O$ (**2**).

## Experimental Section

**Materials.** Malonic acid, basic copper(II) carbonate [$CuCO_3{\cdot}Cu(OH)_2$], and 1,2-bis(4-pyridyl)ethylene were purchased from commercial sources and used as received. Elemental analyses (C, H, N) were performed on an EA 1108 CHNS-O microanalytical analyzer.

**Synthesis of $\{(H_2bpe)[Cu(mal)_2]\}_n{\cdot}4nH_2O$ (1).** Basic copper(II) carbonate (0.221 g, 1 mmol) is allowed to react with malonic acid (0.208 g, 2 mmol) in water (10 cm$^3$) to give an aqueous solution of copper(II) malonate. An ethanolic solution (20 cm$^3$) of bpe (0.364 g, 2 mmol) was mixed with an aqueous solution (10 cm$^3$) of malonic acid (0.208 g, 2 mmol) affording a colorless solution. The copper(II) malonate solution was transferred to a tube, and then, the colorless one was added dropwise. The white solid that was formed at the interface of both solutions redissolved after 2 days leading to a sky blue solution. Large rhombic pale-blue single crystals of **1** were formed after a week. Anal. Calcd for $C_{18}H_{24}N_2O_{12}Cu$: C, 41.25; H, 4.58; N, 5.35. Found: C, 41.4; H, 4.4; N, 6.4. IR (KBr disk/cm$^{-1}$): 1718w, 1629m, 1610vs, 1599vs, 1583vs, 1508m, 1432s, 1379m, 834m, 743m, 551m.

**Synthesis of $[Cu_4(mal)_4(bpe)_3]_n{\cdot}6nH_2O$ (2).** Blue rectangular crystals of **2** were grown by slow diffusion in an H-tube of an aqueous solution of copper(II) and malonate [1:1 molar ratio, 1 mmol of Cu(II)] in one arm and an ethanol/water (50:50 v/v) mixture containing bpe (1 mmol) in the other one. They were collected and air-dried and used for all measurements. Anal. Calcd

---

[3] Yaghi, O. M.; Li, H.; Davis, C.; Richardson, D.; Groy, T. L. *Acc. Chem. Res.* **1998**, *31*, 474.

[4] Hagrman, P. J.; Hagrman, D.; Zubieta, J. *Angew. Chem., Int. Ed.* **1999**, *38*, 2638.

[5] O'Keeffe, M.; Edaoudi, M.; Li, H.; Reineke, T.; Yaghi, O. M. *J. Solid State Chem.* **2000**, *152*, 3.

[6] Braga, D. *J. Chem. Soc., Dalton Trans.* **2000**, *21*, 3705.

[7] Lenh, J.-M. *Supramolecular Chemistry: Concepts and Perspectives*; VCH: Weinheim, Germany, 1995.

[8] Fujita, M.; Kwon, Y. J.; Washizu, S.; Ogura, K. *J. Am. Chem. Soc.* **1994**, *116*, 1151.

[9] For example: Denti, G.; Seroni, S.; Campagna, S. In *Perspectives in Coordination Chemistry*; Williams, A. F., Floriani, C., Eds.; VCH: Weinheim, Germany, 1992; p 153.

[10] Garcia, Y.; Kahn, O.; Rabardel, L.; Chansou, B.; Salñmon, L.; Tuchagues, J. P. *Inorg. Chem.* **1999**, *38*, 4663.

[11] Tangouolis, V.; Raptopolou, C. P.; Psycharis, V.; Terzis, A.; Korda, K.; Perlepes, S. P.; Cador, O.; Kahn, O.; Bakalbassis, E. G. *Inorg. Chem.* **2000**, *39*, 2522.

[12] Rodríguez-Martín, Y.; Hernández-Molina, M.; Delgado, F. S.; Pasán, J.; Ruiz-Pérez, C.; Sanchiz, J.; Lloret, F.; Julve, M. *CrystEngComm* **2002**, *4*, 522.

[13] Ruiz-Pérez, C.; Rodríguez-Martín, Y.; Hernández-Molina, M.; Delgado, F. S.; Pasán, J.; Sanchiz, J.; Lloret, F.; Julve, M. *Polyhedron* **2003**, *22*, 2111.

[14] Pasán, J.; Delgado, F. S.; Rodriguez-Martín, Y.; Hernández-Molina, M.; Ruiz-Pérez, C.; Sanchiz, J.; Lloret, F.; Julve, M. *Polyhedron* **2003**, *22*, 2143.

[15] (a) Hennigar, T. L.; MacQuarrie, D. C.; Losier, P.; Rogers, R. D.; Zaworotko, M. J. *Angew. Chem., Int. Ed. Engl.* **1997**, *36*, 972. (b) Fujita, M.; Kwon, Y. J.; Miyazawa, M.; Ogura, K. *J. Chem. Soc., Chem. Commun.* **1994**, 1977. (c) Real, J. A.; Andres, E.; Munoz, M. C.; Julve, M.; Granier, T.; Bousseksou, A.; Varret, F. *Science* **1995**, *268*, 265.

[16] (a) Lehn, J.-M. *Angew. Chem., Int. Ed. Engl.* **1990**, *29*, 1304. (b) Palmans, A. R. A.; Vekemans, J. A. J. M.; Kooijman, H.; Speck, A. L.; Meijer, E. W. *J. Chem. Soc., Chem. Commun.* **1997**, 2247.

[17] De Munno, G.; Julve, M.; Viau, G.; Lloret, F.; Faus, J.; Vitervo, D. *Angew. Chem., Int. Ed. Engl.* **1996**, *35*, 1807.

**Table 1.** Crystallographic Data for Compounds **1** and **2**

| | **1** | **2** |
|---|---|---|
| formula | $C_{18}H_{24}N_2O_{12}Cu$ | $C_{24}H_{25}N_3O_{11}Cu_2$ |
| fw | 523.9 | 658.5 |
| space group | $P\bar{1}$ | $P2_1/n$ |
| $a$, Å | 4.8831(10) | 13.462(3) |
| $b$, Å | 9.585(2) | 10.275(5) |
| $c$, Å | 11.813(2) | 19.579(4) |
| α, deg | 77.29(3) | 90.0 |
| $\beta$, deg | 82.18(3) | 105.21(3) |
| $\gamma$, deg | 84.92(3) | 90.0 |
| $V$, Å$^3$ | 533.4(2) | 2613.3(10) |
| $Z$ | 1 | 4 |
| $T$ (K) | 293(2) | 293(2) |
| $\rho_{calcd}$ (Mg m$^{-3}$) | 1.6312(6) | 1.6636(6) |
| $\lambda$ (Å) | 0.71073 | 0.71073 |
| $\mu$(Mo Kα) (mm$^{-1}$) | 1.093 | 1.694 |
| $R^a$ | 0.0293 | 0.0794 |
| $R_w{}^b$ | 0.0791 | 0.1576 |

[a] $R = \Sigma||F_o| - |F_c||/\Sigma|F_o|$. [b] $R_w = [[\Sigma w(|F_o|^2 - |F_c|^2)^2]/\Sigma|F_o|^2]^{1/2}$.

for $C_{24}H_{21}N_3O_{11}Cu_2$: C, 44.0; H, 3.2; N, 6.4. Found: C, 43.9; H, 3.7; N, 6.4. IR (KBr disk/cm$^{-1}$): 1642sh, 1609s, 1589vs, 1507w, 1432s, 1365m, 832m, 551m.

**Physical Measurements.** IR spectra of **1** and **2** (4000−400 cm$^{-1}$) were recorded on a Bruker IF S55 spectrometer with the samples prepared as KBr pellets. Variable temperature (2.0−290 K) magnetic susceptibility measurements of crushed crystals of **1** and **2** were carried out in a Quantum Design SQUID magnetometer operating at applied magnetic fields of 100 G ($T < 50$ K) and 1000 G ($T > 50$ K). Diamagnetic corrections of all the constituent atoms were estimated from Pascal's constants[18] as $-259 \times 10^{-6}$ and $-319 \times 10^{-6}$ cm$^3$ mol$^{-1}$ for **1** and **2**, respectively. Magnetic susceptibility data were also corrected for the temperature-independent paramagnetism [$60 \times 10^{-6}$ cm$^3$ mol$^{-1}$ per copper(II) ion] and the magnetization of the sample holder.

**Crystal Data Collection and Structure Determination.** Crystal data and details of the refinement for compounds **1** and **2** are listed in Table 1. Diffraction intensities for **1** were collected at 293 K on a Bruker Smart CCD, whereas data for **2** were collected on an Enraf-Nonius MACH3 four-circle diffractometer. Both diffractometers were equipped with a graphite-monochromated Mo Kα radiation ($\lambda = 0.71073$ Å). All calculations for data reduction, structure solution, and refinement were done by standard procedures (WINGX).[19] The structures of all compounds were solved by direct methods using SHELXS97.[20a] All non-hydrogen atoms were refined anisotropically by full-matrix least-squares techniques on $F^2$ by using the SHELXL97[20b] computational program. The hydrogen atoms for malonate and bpe atoms of **1** were set in calculated positions and isotropically refined as riding atoms. The hydrogen atoms of **2** were located from difference maps and refined with isotropic temperature factors. The final geometrical calculations and the graphical manipulations were carried out with PARST97,[21] PLATON,[22] and CRYSTAL MAKER[23] programs. Selected bond distances and angles for **1** and **2** are listed in Tables 2 and 3, respectively.

## Results and Discussion

**Table 2.** Selected Bond Lengths (Å) and Angles (deg) for **1**

| | | | |
|---|---|---|---|
| Cu1−O1 | 1.9314(11) | Cu1−O2 | 1.9367(10) |
| Cu1−O3$^c$ | 2.6107(14) | | |
| O1−Cu1−O2 | 93.88(5) | O1−Cu1−O2$^a$ | 86.12(5) |
| O1−Cu1−O3$^c$ | 91.25(5) | O1−Cu1−O3$^b$ | 88.75(5) |
| O2−Cu1−O3$^c$ | 93.60(5) | O2−Cu1−O3$^b$ | 86.40(5) |
| O1$^a$−Cu1−O3$^c$ | 88.75(5) | | |

[a] $-x, -y, -z$. [b] $x - 1, y, z$. [c] $-x + 1, -y, -z$.

**Table 3.** Selected Bond Lengths (Å) and Angles (deg) for **2**

| | | | |
|---|---|---|---|
| Cu1−O4 | 1.940(2) | Cu1−O33$^a$ | 1.968(2) |
| Cu1−N1 | 2.080(2) | Cu1−N2 | 2.029(2) |
| Cu1−O33 | 2.370(2) | | |
| Cu2−O1 | 1.980(2) | Cu2−O2 | 1.979(2) |
| Cu2−O32$^b$ | 1.957(2) | Cu2−N3 | 2.022(3) |
| Cu2−O31$^b$ | 2.278(2) | Cu2−O34$^c$ | 2.627(3) |
| O4−Cu1−N1 | 85.94(9) | O33$^a$−Cu1−N1 | 91.06(9) |
| O4−Cu1−N2 | 91.78(9) | O33$^a$−Cu1−N2 | 91.44(9) |
| O4−Cu1−O33$^a$ | 175.25(8) | N1−Cu1−N2 | 175.79(10) |
| O4−Cu1−O33 | 99.73(8) | O33$^a$−Cu1−O33 | 76.79(8) |
| N1−Cu1−O33 | 94.24(8) | N2−Cu1−O33 | 89.63(8) |
| O1−Cu2−O2 | 88.42(8) | O32$^b$−Cu2−N3 | 88.71(10) |
| O1−Cu2−O32$^b$ | 94.49(9) | O1−Cu2−N3 | 176.50(9) |
| O2−Cu2−N3 | 88.24(9) | O2−Cu2−O32$^b$ | 172.89(9) |
| O1−Cu2−O31$^b$ | 92.08(9) | O1−Cu2−O34$^c$ | 95.02(9) |
| O2−Cu2−O31$^b$ | 98.63(9) | O2−Cu2−O34$^c$ | 88.22(9) |
| O32$^b$−Cu2−O31$^b$ | 87.77(8) | O32$^b$−Cu2−O34$^c$ | 85.07(9) |
| N3−Cu2−O31$^b$ | 89.45(9) | N3−Cu2−O34$^c$ | 83.85(10) |
| O31$^b$−Cu2−O34$^c$ | 170.30(9) | | |

[a] $-x + 1, -y + 2, -z$. [b] $x, y - 1, z$. [c] $-x + 1.5, y - 0.5, -z + 0.5$.

**Description of the Structures. $\{(H_2bpe)[Cu(mal)_2]\}_n \cdot 4nH_2O$ (1).** The structure of complex **1** is made up of $[Cu(mal)_2]^{2-}$ anions, $H_2bpe^{2+}$ cations, and crystallization water molecules (Figure 1). The anionic units are linked through axial copper to carboxylate-oxygen bonds leading to uniform copper(II) chains which run parallel to the $x$-axis (Figure 2). Each chain is weakly interconnected through hydrogen bonds involving noncoordinated water molecules [2.833(3) and 2.725(3) Å for O(1w)···O(2w) and O(2w)···O(1wd), respectively; (d) = $x - 1, y, z$], malonate oxygen atoms [2.847(3) and 2.787(2) Å for O(3)···O(1w) and O(3e)···O(2w), respectively; (e) = $-x + 1, -y + 1, -z$], and protonated-bpe nitrogen atoms [2.669(2) Å for O(4f)···N(1); (f) = $-x, -y, -z + 1$].

The copper(II) atoms are surrounded by six oxygen atoms from four different malonate groups forming an elongated octahedral environment with geometric values $\phi = 53.86°$ and $s/h = 1.52$ ($\phi$ and $s/h$ being the twist angle and compression ratio, respectively).[24] Four coplanar oxygen atoms from two bidentate malonate ligands build the equatorial plane around the copper atom, while the apical positions are filled by two carboxylate oxygen atoms from two neighboring $[Cu(mal)_2]^{2-}$ units. The mean value of the equatorial Cu−O bond distances is 1.9341(11) Å, and the angle subtended at the copper atom by the malonate ligand [O(1)−Cu(1)−O(2)] is 93.88(5)°. These structural parameters are within the range observed in previous malonate-containing copper(II) complexes.[25] The value of the apical Cu−O bond length [2.6107(14) Å for Cu(1)−O(3c)] is significantly longer than the equatorial ones.

---

(18) Earshaw, A. *Introduction to Magnetochemistry*; Academic Press: London, 1968.

(19) Farrugia, L. J. *J. Appl. Crystallogr.* **1999**, *32*, 837.

(20) (a) Sheldrick, G. M. *SHELXS-97, Program for Crystal Structure Solution*; University of Göttingen: Göttingen, Germany, 1997. (b) Sheldrick, G. M., *SHELXL-97, Program for Crystal Structure Refinement*; University of Göttingen: Göttingen, Germany, 1997.

(21) Nardelli, M. *J. Appl. Crystallogr.* **1995**, *28*, 659.

(22) Spek, A. L. *PLATON, Molecular Geometry Program*; University of Utrecht: Utrecht, The Netherlands, 1999.

(23) *Crystal Maker 4.2.1*; CrystalMaker Software: Bicester, U.K.

(24) Stiefel, E. I.; Brown, G. F. *Inorg. Chem.* **1972**, *11*, 434.

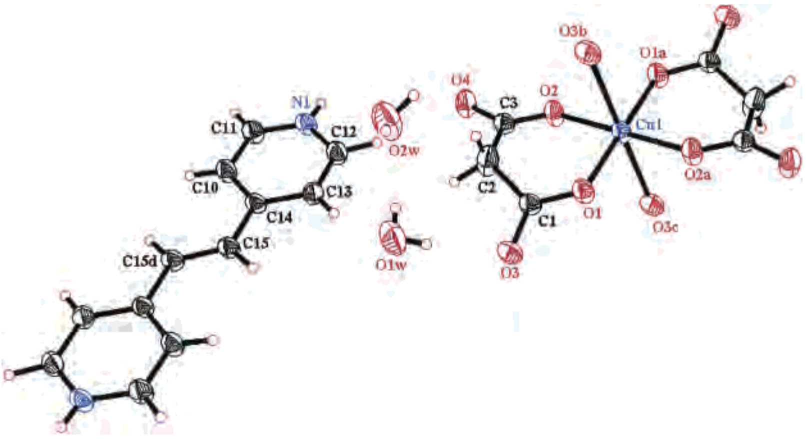

**Figure 1.** Perspective view of the $[Cu(mal)_2]^{2-}$ and $H_2bpe^{2+}$ units of compound **1** with the atom numbering. Thermal ellipsoids are drawn at the 50% probability level.

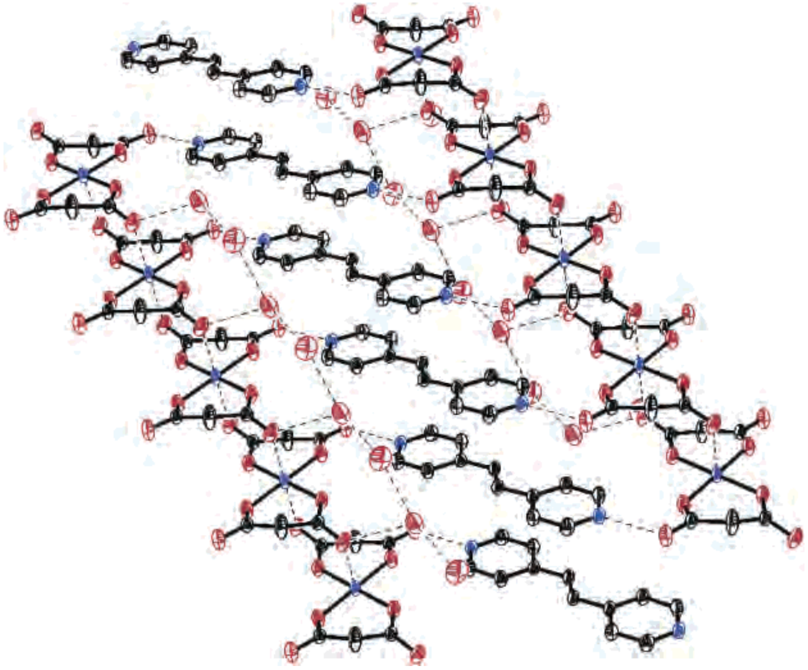

**Figure 2.** View of the arrangement of the malonato−copper(II) chains and $H_2bpe^{2+}$ units of **1** along the *x* axis. Hydrogen bonds are ilustrated by dashed lines.

Each malonate group acts simultaneously as a monodentate [through O(3) toward Cu(1g); (g) = $x + 1, y, z$] and bidentate [through O(1) and O(2) toward Cu(1)] ligand, and it exhibits a twist-boat conformation with $\theta = 82.4(2)°$, $\phi = 94.5(2)°$, and $Q_T = 0.3557(15)$ Å ($\phi$ and $Q_T$ being the phase angle and total puckering amplitude, respectively).[26] The values of the C−C [1.507(2)−1.512(2) Å] and C−O [1.2471(15)−1.261(2) Å] malonate bond distances and O−C−O [122.18(11)−123.37(12)°] malonate bond angles agree well with those previously observed in other malonate-containing copper(II) complexes.[25] Within the uniform copper(II) chain, the carboxylate-bridge exhibits the *anti*−*syn* conformation, and it connects an equatorial site of one copper atom with an apical site of the adjacent copper atom. The copper−copper separation through this carboxylate-bridge is 4.8831(10) Å [Cu(1)⋯Cu(1c); (c) = $-x + 1, -y, -z$], whereas the shortest interchain copper−copper distances are 9.585(2) Å [Cu(1)⋯Cu(1h); (h) = $x, y + 1, z$] and 11.813(2) Å [Cu(1)⋯Cu(1i); (i) = $x, y, z + 1$].

---

(25) Malonate containing Cu(II) complexes: (a) Chattopadhyay, D.; Chattopadhyay, S. K.; Lowe, P. R.; Schwalbe, C. H.; Mazumder, S. K.; Rana, A.; Ghosh, S. *J. Chem. Soc., Dalton Trans.* **1993**, 913. (b) Gil de Muro, I.; Mautner, F. A.; Insausti, M.; Lezama, L.; Arriortua, M. I.; Rojo, T. *Inorg. Chem.* **1998**, *37*, 3243. (c) Ruiz-Pérez, C., Sanchiz, J.; Hernández-Molina, M.; Lloret, F.; Julve, M. *Inorg. Chim. Acta* **2000**, *298*, 245−250. (d) Ruiz-Pérez, C.; Sanchiz, J.; Hernández-Molina, M.; Lloret F.; Julve, M. *Inorg. Chem.* **2000**, *39*, 1363. (e) Ruiz-Pérez, C.; Hernández-Molina, M.; Lorenzo-Luis, P.; Lloret, F.; Cano, J.; Julve, M. *Inorg. Chem.* **2000**, *39*, 3845. (f) Ruiz-Pérez, C.; Sanchiz, J.; Hernández-Molina, M.; Lloret, F.; Julve, M. *Inorg. Chim. Acta* **2000**, *298*, 245. (g) Rodríguez-Martín, Y.; Sanchiz, J.; Ruiz-Pérez, C.; Lloret, F.; Julve, M. *Inorg. Chim. Acta* **2001**, *326*, 20. (h) Rodríguez-Martín, Y.; Ruiz-Pérez, C.; Sanchiz, J.; Lloret, F.; Julve, M. *Inorg. Chim. Acta* **2001**, *318*, 159. (i) Sanchiz, J.; Rodróguez-Martín, Y.; Ruiz-Pérez, C.; Mederos, A.; Lloret, F.; Julve, M. *New J. Chem.* **2002**, *26*, 1624. (j) Rodríguez-Martín, Y.; Hernández-Molina, M.; Delgado, F. S.; Pasán, J.; Ruiz-Pérez, C.; Sanchiz, J.; Lloret, F.; Julve, M. *CrystEngComm* **2002**, *4*, 440. (k) Sain, S.; Maji, T. K.; Mostafa, G.; Lu, T. H.; Chanduri, N. R. *New J. Chem.* **2003**, *27*, 185.

(26) Cremer, D.; Pople, J. A. *J. Am. Chem. Soc.* **1975**, *97*, 1354.

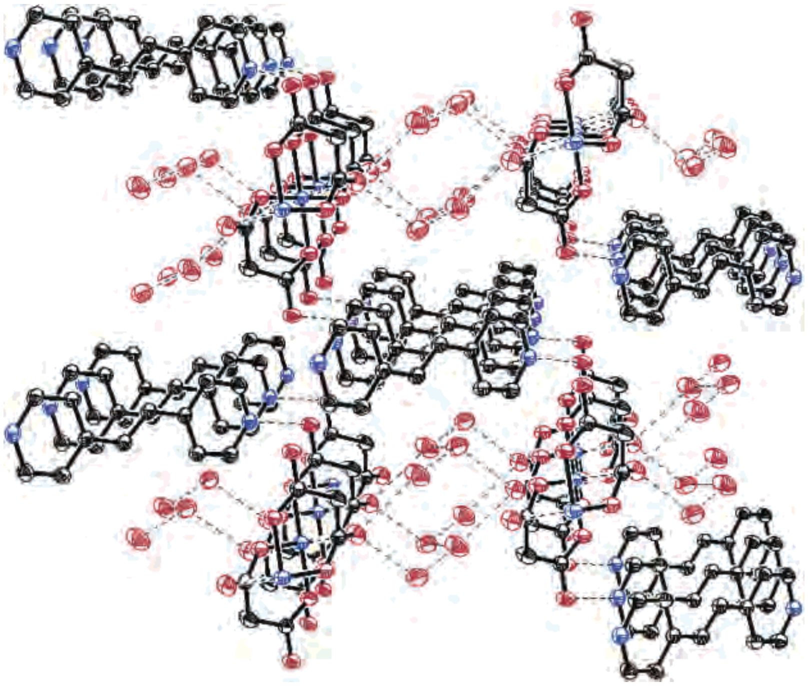

**Figure 3.** View of the stacking of malonato−copper(II) chains and $H_2bpe^{2+}$ units of **1** down the *x* axis.

The protonated $H_2bpe^{2+}$ unit is planar, and it exhibits the *trans*-conformation. These structural features were previously observed in the free[27] and coordinated[28] bpe molecules. Bond lengths and angles of the $H_2bpe^{2+}$ agree well with those reported for the neutral bpe ligand.[27] The $H_2bpe^{2+}$ units are stacked along the *a*-axis in an eclipsed conformation (Figure 3). The value of the distance between planes of adjacent $H_2bpe^{2+}$ units along this direction is 4.8831(10) Å revealing that $\pi-\pi$ type interactions are negligible. Bpe ligand in **1** exhibits an eclipsed arrangement along the *a*-axis (Figure 3). This type of stacking is most likely imposed by the protonation of bpe ligand and the extensive hydrogen bonding associated with it (see earlier remarks).

**$[Cu_4(mal)_4(bpe)_3]_n \cdot 6nH_2O$ (2).** Complex **2** has a three-dimensional structure involving corrugated layers of malonato-bridged copper(II) ions (Figure 4a), which are linked by bis-monodentate bpe molecules (Figure 4b). The layers are stacked along the $[\bar{1}01]$ direction, and the bis-monodentated bpe ligands run parallel to the $[\bar{1}01]$ and [100] directions exhibiting a T-shape arrangement. The asymmetric unit along with the atom numbering is shown in Figure 5.

Two crystallographically independent copper(II) ions noted Cu(1) (Figure 6a) and Cu(2) (Figure 6b) occur in **2**. Cu(1) exhibits a $CuN_2O_3$ slighty distorted square-pyramidal environment, the $\tau$ value being 0.009 (square-pyramidal and trigonal-pyramidal surroundings correspond to $\tau = 0$ and $\tau = 1$, respectively).[29] Cu(2) is six-coordinated $CuNO_5$ and has a 4 + 1 + 1 distorted octahedral conformation with $\phi = 54.69°$ and $s/h = 1.40$.[24] The basal sites around Cu(1) are occupied by two bpe-nitrogen atoms and two carboxylate-oxygen atoms from two different malonate ligands. The Cu−N bond lengths [average value 2.055(2) Å] are somewhat longer than the Cu−O ones [mean value 1.954(2) Å]. The apical position is occupied by a malonate-oxygen atom [2.370(2) Å for Cu(1)−O(33)]. The equatorial plane around Cu(2) is built by a bpe-nitrogen atom and three carboxylate-oxygen atoms from two different malonate groups [the average value of Cu−N and mean Cu−O bonds being 2.022(3) and 1.972(2) Å, respectively]. These values are in good agreement with those observed in previously reported structures of malonate-[25] and bpe-containing[28] copper(II) complexes. Apical positions at Cu(2) are ocupied by two structurally different malonate-oxygen atoms [2.278(2) and 2.627(3) Å for Cu(2)−O(31b) and for Cu(2)−O(34c), respectively; (b) = *x*, *y* − 1, *z*]. The longer axial Cu(2)−O bond corresponds to the monodentate malonate ligand whereas the shorter one comes from the bidentate malonate.

The malonate ligands in **2** exhibit two different coordination modes. One malonate acts simultaneously as a monodentate [through O(4) toward Cu(1)] and bidentate [through O(1), O(2) toward Cu(2)] ligand exhibiting the *anti*−*syn* conformation. It has the six-membered ring twist-boat conformation [$\theta = 97.2(2)°$, $\phi = 107.9(2)°$].[26] The other malonate ligand bridges four copper atoms; it adopts simultaneously the tris-monodentate [O(34) toward Cu(2f) and O(33) toward Cu(1) and Cu(1a); (a) = $-x + 1$, $-y + 2$, $-z$, (f) = $-x + 1.5$, $y + 0.5$, $-z + 0.5$] and bidentate

---

[27] Vansant, J.; Smets, G.; Declercq, J. P.; Germain, G.; van Meerssche, M. *J. Org. Chem.* **1980**, *45*, 1557.

[28] Bpe containing copper(II) complexes: (a) Lu, J. Y.; Babb, A. M. *Inorg. Chem.* **2001**, *40*, 3261. (b) Zhang, H.-X.; Kang, H.-X.; Zhou, Z.-Y.; Chan, A. S. C.; Chen, Z.-N.; Ren, C. *J. Chem. Soc., Dalton Trans.* **2001**, 1664. (c) Carlucci, L.; Ciani, G.; Proserpi, D. M.; Rizzato, S. *Chem. Commun.* **2001**, 1198. (d) Hagrman, D.; Haushalter, R. C.; Zubieta, J. *Chem. Mater.* **1998**, *10*, 361. (e) Hagrman, D.; hammond, R. P.; Haushalter, R.; Zubieta, J. *Chem. Mater.* **1998**, *10*, 2091. (f) Carlucci, L.; Ciani, G.; Gramaccioli, A.; Proserpio, D. M.; Rizzato, S. *CrystEngComm* **2000**, 29. (g) Visinescu, D.; Andruh, M.; Muller, A.; Schmidtmann, M.; Journaux, Y. *Inorg. Chem. Commun.* **2002**, *5*, 42.

[29] Addison, A. W.; Rao, T. N.; Reedijk, J.; van Rijn, J.; Verschoor, G. C. *J. Chem. Soc., Dalton Trans.* **1984**, 1349.

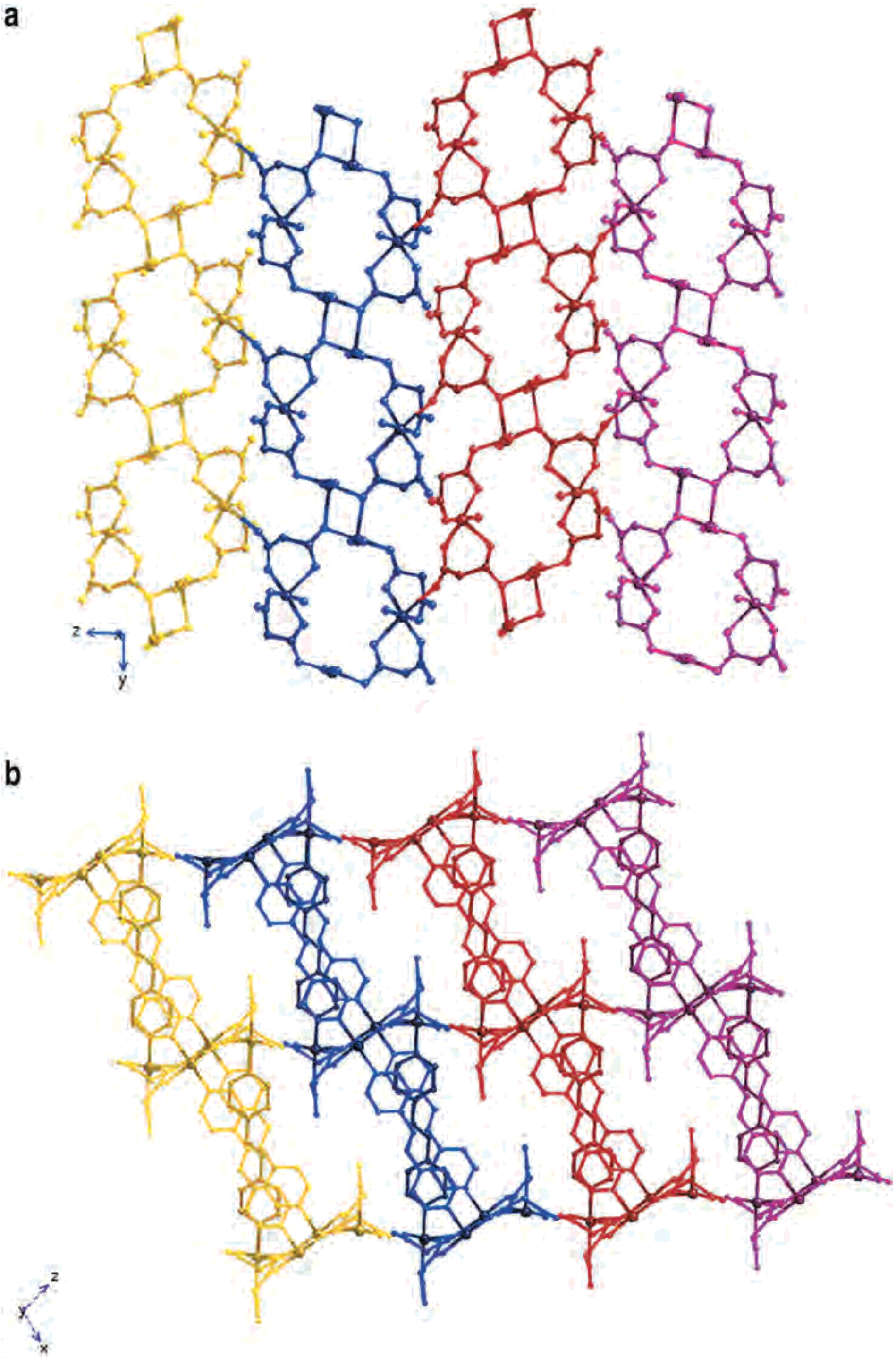

**Figure 4.** Perspective views of (a) the malonato-bridged copper(II) corrugated plane and (b) its polymerization through bis-monodentate bpe in **2**.

[through O(32) and O(31) toward Cu(2e); (e) = $x$, $y + 1$, $z$] coordination modes, and it exhibits a boat conformation [$\theta = 85.5(5)°$ and $\phi = 121.3(2)°$].[26] The carboxylate bridges of this latter malonate show the *anti*−*syn* [Cu(2)−O(31b)−C(30b)−O(33b)−Cu(1d); (d) = $-x + 1$, $-y + 1$, $-z$] and *anti*−*anti* [Cu(2)−O(31b)−C(30b)−O(33b)−Cu(1b)] conformations. The bond lengths and angles of the two malonate ligands are in good agreement with those previously reported for malonate-containing copper(II) complexes.[25]

Within the malonate-bridged copper(II) layers, one can distinguish (Figure 7) tetranuclear units linked by double $\mu$-oxo and single carboxylate bridges. Each tetranuclear unit forms a 16-membered ring [Cu(1)−O−C−O−Cu(2)]$_4$ with the four copper atoms located at the corners of a quasiplanar parallelogram. Two different carboxylate-bridges are present in the tetranuclear unit: the equatorial−equatorial and the equatorial−axial linking pathways which lead to Cu(1)···Cu(2) separations of 5.0082(10) and 4.9488(11) Å, respectively. Each tetranuclear unit, within the layer, is linked to six other ones through two $\mu$-oxo- [connecting Cu(1) atoms] and four carboxylate-bridges [linking Cu(2) atoms]. Each Cu(1) atom is connected to another Cu(1) from a different

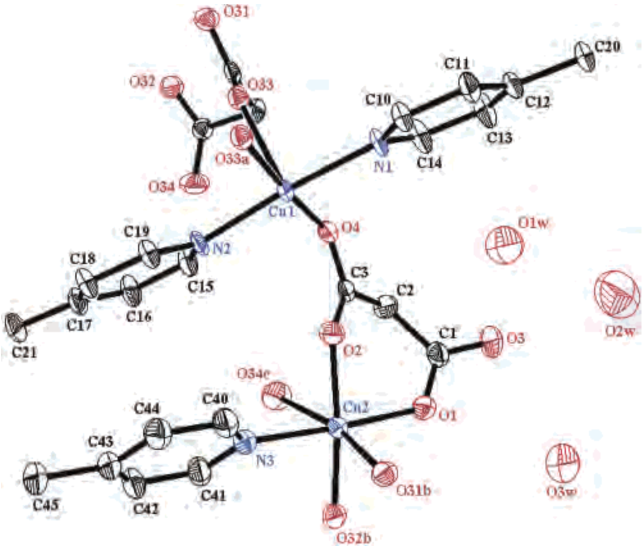

**Figure 5.** Perspective view of the asymmetric unit of **2**. Hydrogen atoms are omitted for simplicity. Thermal ellipsoids are drawn at the 50% probability level.

tetranuclear unit through a double $\mu$-oxo bridge [103.21(8)° for Cu(1)−O−Cu(1a)] with Cu(1)···Cu(1a) separation of 3.4095(7) Å. Each oxygen-oxo atom occupies an apical site at one copper atom and a basal site at the other one. Each Cu(2) is linked to two other Cu(2) atoms from two different tetranuclear units through single carboxylate bridges exhibiting the *anti*−*syn* conformation, the copper−copper separation being 6.5268(13) Å [Cu(2)···Cu(2c)]. This carboxylate group exhibits the apical−equatorial bridging pathway.

The bpe molecule exhibits the *trans*-conformation, and it acts as a bis-monodentate ligand connecting the corrugated layers of malonate-bridged copper(II) ions. The shortest interlayer separations across bridging bpe are 13.462(3) Å [Cu(1)···Cu(1h); (h) = $x + 1$, $y$, $z$] and 13.406(2) Å [Cu(2)···Cu(2g); (g) = $-x + 2$, $-y + 1$, $-z$]. These values are within the range reported in previous bpe-bridged copper(II) complexes.[28]

**Magnetic Properties.** The magnetic behavior of **1** in the form of a $\chi_M T$ versus $T$ plot [$\chi_M$ being the magnetic susceptibility per one copper(II) ion] is shown in Figure 8. $\chi_M T$ at 290 K is equal to 0.39 cm$^3$ mol$^{-1}$ K, a value which is as expected for a magnetically isolated spin doublet. Upon cooling, $\chi_M T$ remains practically constant up to 50 K, and then, it increases smoothly at lower temperatures, reaching a value of 0.43 cm$^3$ mol$^{-1}$ K at 2.0 K. This curve reveals the occurrence of an overall weak ferromagnetic interaction. As the structure of **1** is made up of uniform chains of $[Cu(mal)_2]_n^{2n-}$ units which are well separated from each other by large $(H_2bpe)^{2+}$ cations, its magnetic data can be analyzed through the numerical expression for a ferromagnetically coupled regular chain of local spin doublets.[30] Least-squares fit of the magnetic data leads to $J = +0.049(1)$ cm$^{-1}$ and $g = 2.062(2)$.

An inspection of the structure of **1** allows us to account for the observed weak ferromagnetic coupling. The unpaired electron of Cu(1) in the elongated six-coordinated environment is mainly located in the equatorial plane, and it is of the $d_{x^2-y^2}$ type (magnetic orbital) [the $x$ and $y$ axes being roughly defined by the Cu(1)−O(1) and Cu(1)−O(2) bonds]. A weak spin density is thus expected in the apical positions (see Scheme 1). As the intrachain exchange pathway in **1** involves the equatorial−apical connection through a carboxylate bridge [Cu(1)−O(1)−C(1)−O(3)···Cu(1g)], the overlap ($S$) between the magnetic orbitals of Cu(1) and Cu(1g) is predicted to be very small or zero (accidental orthogonality). Given that the magnitude of the antiferromagnetic interaction in a copper(II) dimer is proportional to $S$,[2,31] the ferromagnetic contribution is expected to be

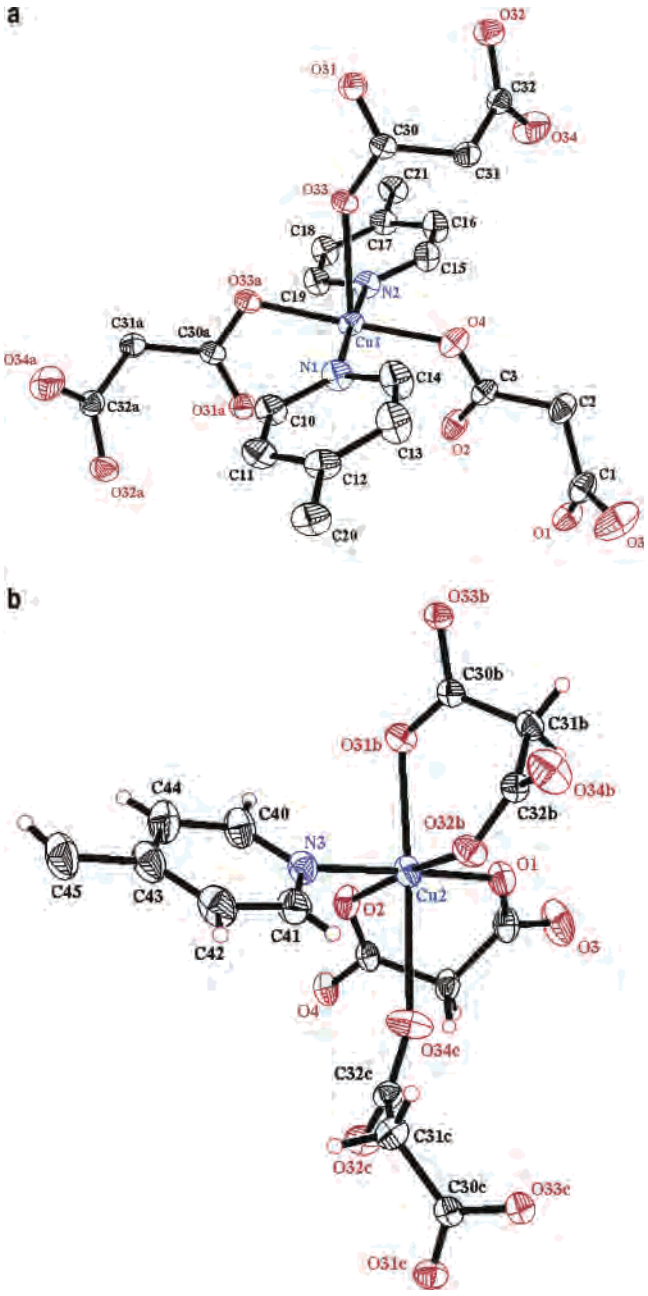

**Figure 6.** Perspective views of the two crystallographically independent copper atoms (a) Cu(1) and (b) Cu(2) of **2**.

---

(30) Baker, G. A., Jr.; Rushbrooke, G. S.; Gilbert, H. E. *Phys. Rev.* **1964**, *135*, A1272.

(31) Kahn, O. In *Molecular Magnetism*; VCH: New York, 1993 and references therein.

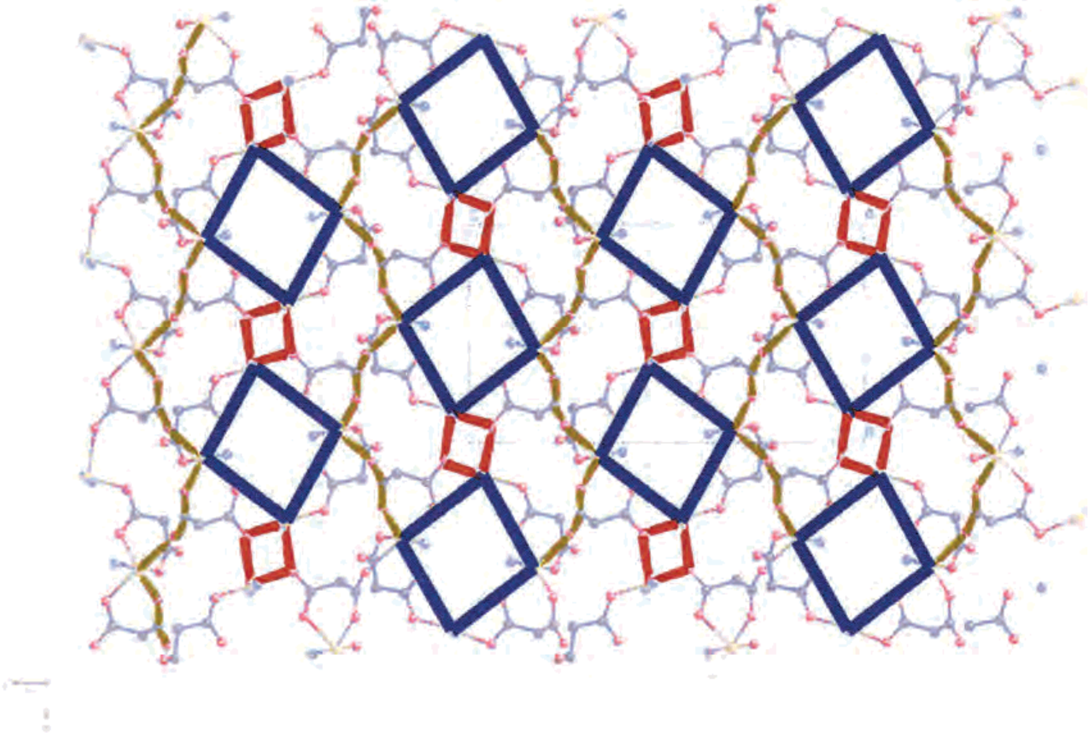

**Figure 7.** Tetranuclear copper(II) motifs (blue) connected through Cu(1) by double $\mu$-oxo groups (red) and through Cu(2) by malonate−carboxylate bridges (yellow).

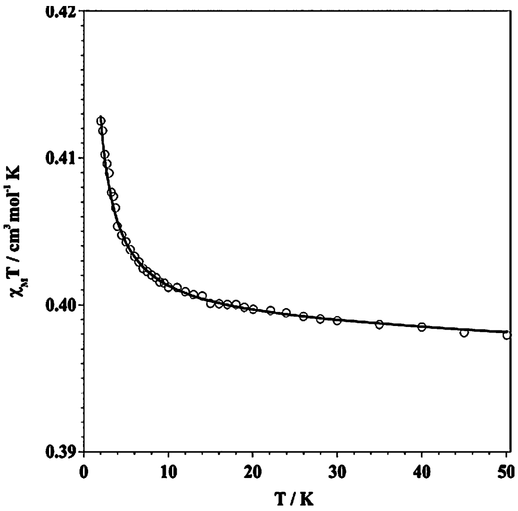

**Figure 8.** Temperature dependence of the $\chi_M T$ product of **1**: (○) experimental data and (—) best fit curve (see text).

**Scheme 1**

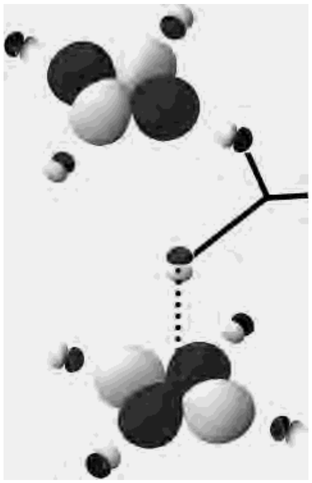

dominant, and the resulting magnetic coupling in **1** is most likely ferromagnetic, as observed. In fact, previous experimental and theoretical studies of carboxylato-bridged copper(II) complexes have shown that the value of the exchange coupling between copper(II) ions through bridging carboxylate ($J$) is strongly dependent on the bridging mode of the carboxylate (*syn*−*syn*, *anti*−*anti*, and *anti*−*syn*) and the type of Cu−O−C−O−Cu pathway involved (equatorial−equatorial or equatorial−apical).[14,25h,32] Finally, the value of the ferromagnetic coupling observed in compound **1** ($J$ = +0.049(1) cm$^{-1}$) is very small compared with that of other compounds with similar orientations of the bridge and magnetic orbitals such as [$Cu_2(mal)_2(H_2O)_6$] ($J$ = +1.8 cm$^{-1}$),[25a] {[$Cu(H_2O)_3$][$Cu(mal)_2(H_2O)$]}$_n$ ($J$ = +1.9 cm$^{-1}$),[25d] [$Cu(Im)_2(mal)$]$_n$ ($J$ = +1.64 cm$^{-1}$),[25i] and [$Cu(2\text{-}MeIm)_2(mal)$]$_n$ ($J$ = +0.39 cm$^{-1}$)[25i] (Im = imidazole and 2-MeIm = 2-methylimidazole). This is mainly due to the somewhat greater value of the apical Cu(1)···O(malonate) distance in **1** (2.611 Å) compared with those observed in the related compounds (less than 2.39 Å).

The magnetic properties of **2** in the form of $\chi_M T$ versus $T$ plot [$\chi_M$ being the magnetic susceptibility per four Cu(II) ions] are shown in Figure 9. $\chi_M T$ at 290 K is 1.5 cm$^3$ mol$^{-1}$ K, a value which corresponds to that expected for four

---

[32] (a) Cano, J.; Alemany, P.; Alvarez, S.; Verdaguer, M.; Ruiz, E. *Chem. Eur. J.* **1998**, *4*, 476. (b) Cabrero, J.; Ben Amor, N.; de Graaf, C.; Illas, F.; Caballol, R. *J. Phys. Chem.* **2000**, *104*, 9983. (c) Castillo, O.; Luque, A.; Lloret, F.; Julve, M.; Roman, P. *Inorg. Chim. Acta* **2001**, *315*, 9. (d) Castillo, O.; Luque, A.; Lloret, F.; Roman, P. *Inorg. Chim. Acta* **2001**, *324*, 141.

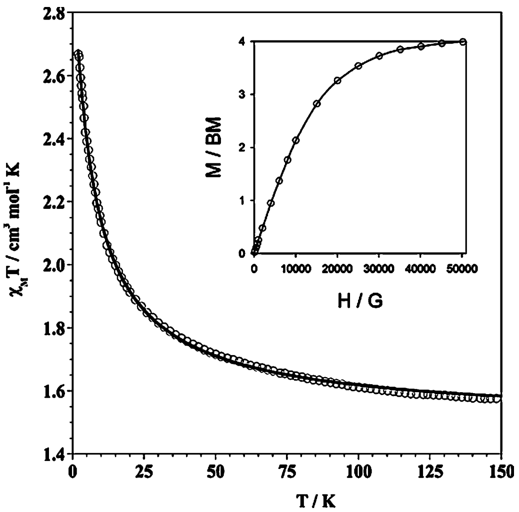

**Figure 9.** Temperature dependence of the $\chi_M T$ product of **2**: (○) experimental data and (—) best fit curve through eq 6 (see text).

magnetically isolated copper(II) ions. Upon cooling, this value continuously increases to reach a value of 2.66 cm$^3$ mol$^{-1}$ K at 2 K. The shape of the curve is indicative of the occurrence of an overall ferromagnetic coupling in **2**.

The structure of **2** consists of $\{Cu(mal)\}_n$ corrugated layers interconnected through bpe ligands to give a 3D framework. From a magnetic point of view, this is a very complicated system, since seven different exchange pathways can be operative: five within the $\{Cu(mal)\}_n$ layers ($J_1$−$J_5$ through carboxylate and double $\mu$-oxo bridges, see Scheme 2), and the other two through the two bpe bridges that connect the layers. It is clear that the much larger copper−copper separations across bridging bpe (more than 13 Å) when compared to the shorter values across double $\mu$-oxo [3.4095(7) Å] and carboxylate bridges [values ranging from 4.9488(11) to 6.5285(13) Å] allow us to discard the exchange pathways through bpe. Thus, the magnetic behavior of **2** can be explained by considering only the exchange pathways within the layer. Focusing on the layer, we have two different copper(II) ions. The links of Cu(2) with its nearest neighbors are depicted in Scheme 2a. One can see there four different exchange pathways ($J_1$−$J_4$) through the carboxylate bridges: (i) equatorial positions at both Cu(1) and Cu(2) atoms are involved in $J_1$; (ii) $J_2$ concerns an axial position at Cu(2) and a basal position at Cu(1d); (iii) $J_3$ involves an axial position at Cu(2) and an apical at Cu(1b); (iv) finally, $J_4$ deals with two different symmetry related Cu(2) atoms connecting an axial position at Cu(2) and an equatorial one at Cu(2f). An additional double $\mu$-oxo bridge between Cu(1) and Cu(1a) atoms (exchange pathway corresponding to $J_5$) is illustrated by Scheme 2b.

**Table 4.** Selected Magneto-Structural Data for Some Carboxylate(malonate)-Bridged copper(II) Complexes

| compd[a] | carboxylate pathway | $J$[b] (cm$^{-1}$) | ref |
|---|---|---|---|
| $[Cu(H_2O)_4][Cu(mal)_2(H_2O)_2]$ | equatorial−apical | +1.8 | 25d |
| $\{[Cu(H_2O)_4]_2[Cu(mal)_2(H_2O)]\}$ | equatorial−apical | +1.2 | 25d |
| $\{[Cu(H_2O)_3][Cu(mal)_2(H_2O)]\}_n$ | equatorial−apical | +1.9 | 25d |
| $[Cu(Im)_2(mal)]_n$ | equatorial−apical | +1.6 | 25i |
| $[Cu(2\text{-}MeIm)_2(mal)]_n$ | equatorial−apical | +0.4 | 25i |
| **1** | equatorial−apical | +0.049 | |
| **2** | equatorial−apical | +6.5 | |
| $\{[Cu(H_2O)_3][Cu(mal)_2(H_2O)]\}_n$ | equatorial−equatorial | +3.0 | 25d |
| $\{[Cu(bpy)(H_2O)][Cu(bpy)(mal)(H_2O)]\}(ClO_4)_2$ | equatorial−equatorial | +4.6 | 25e |
| $[Cu_4(mal)_4(2,4'\text{-}bpy)_4(H_2O)_4]\cdot 8H_2O$ | equatorial−equatorial | +12.3 | 12 |
| $[Cu_2(mal)_2(H_2O)_2(4,4'\text{-}bpy)]$ | equatorial−equatorial | +12.4 | 25h |
| $[\{Cu_3(mal)_2(bpe)_3(H_2O)_2\}(NO_3)_2]_n$ | equatorial−equatorial | +22 | 25k |
| **2** | equatorial−equatorial | +23 | |

[a] Abbreviations used: Im = imidazole, 2-MeIm = 2-methylimidazole, bpy = 2,2′-bipyridine, 2,4′-bpy = 2,4′-bipyridine, and 4,4′-bpy = 4,4′-bipyridine. [b] Values of the magnetic coupling.

Keeping in mind these considerations, a rigorous description of the magnetic structure of **2** would require at least the evaluation of the five exchange coupling parameters. As there is no model to analyze such a complicated magnetic system, we have introduced several approximations that allowed us to determine the values for the main coupling constants and to check further their reliability by comparing them with those already known for this exchange pathways in lower nuclearity malonato-bridged copper(II) complexes.[25] In this respect, and having in mind the overall path length via carboxylate bridges (Scheme 2a,b), the only relevant magnetic interactions are $J_1$ and $J_2$, the remaining ones being neglected in a first approach. So, we are dealing with a model of rectangles with alternating $J_1$ and $J_2$ parameters in the edges (blue motif in Figure 7). The corresponding spin Hamiltonian for this simplified model is given by eq 1:

$$H = -[J_1(S_1S_2 + S_{1A}S_{2A}) + (J_2(S_1S_{2A} + S_{1A}S_2)] \qquad (1)$$

The theoretical expression for the magnetic susceptibility of the tetranuclear complex[33] derived through this Hamiltonian considering an average $g$ value is then

$$\chi_M = \frac{2Ng^2\beta^2}{kT} \frac{[5\exp(Q/kT + R]}{[5\exp(Q/kT) + 3R + \exp((S - Q)/kT) + \exp(-(S + Q)/kT)]} \qquad (2)$$

$$Q = (J_1 + J_2)/2 \qquad (3)$$

$$R = \exp((J_1 - J_2)/2kT) + \exp((J_2 - J_1)/2kT) + \exp(-(J_1 - J_2)/2kT) \qquad (4)$$

$$S = (J_1^{\,2} + J_2^{\,2} - J_1J_2)^{1/2} \qquad (5)$$

In order to take into account the interaction between tetranuclear units, a Weiss constant was introduced [eq 6]:

$$\chi' = \frac{\chi}{1 - (2zJ'/Ng^2\beta^2)\chi} \qquad (6)$$

Least-squares fit of the magnetic data leads to the following parameters: $J_1 = +23(1)$ cm$^{-1}$, $J_2 = +6.5(1)$ cm$^{-1}$, $zJ' = -1.0(1)$ K, and $g = 2.002(2)$. The calculated curve matches the magnetic data in the whole temperature range well.

Let us analyze and compare the values of the coupling constants in **2**. Relevant magneto-structural data for carboxylate(malonate)-bridged copper(II) complexes are listed in Table 4. One can see there that the magnetic coupling between copper(II) ions through the carboxylate(malonate)-

**Scheme 2**

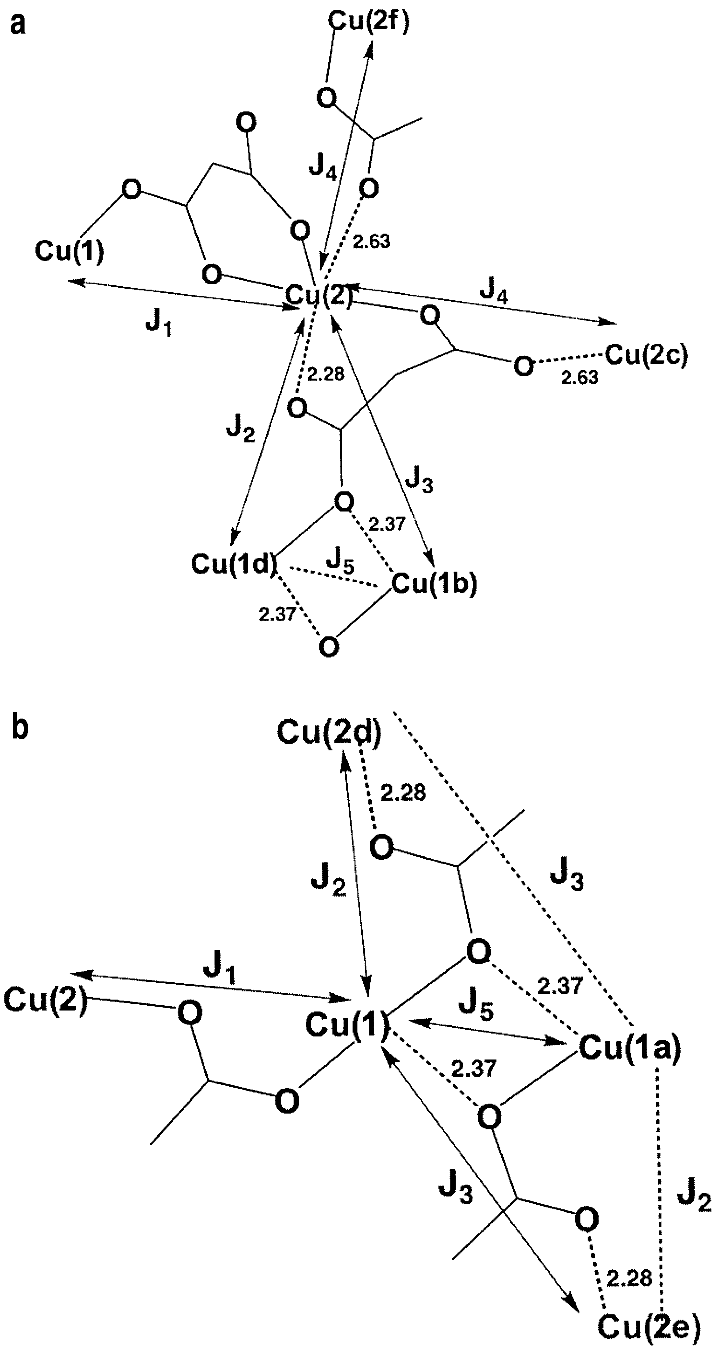

**Scheme 3**

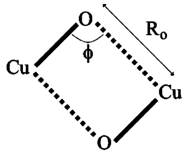

bridge is always ferromagnetic and also that the values through the equatorial−apical exchange pathway are smaller than those corresponding to the equatorial−equatorial ones, as expected. The values of $J_1$ and $J_2$ in **2** are in agreement with these observations, and they are the upper limits of both families. Concerning the value of $J_5$, a few studies involving Cu(II) ions bridged by a double $\mu$-oxo bridges in an out-of-plane exchange pathway (Scheme 3) have been reported, and weak ferro- and antiferromagnetic interactions were observed (values of $J$ ranging from $-4.30$ to $+$ 1.26 $\text{cm}^{-1}$).[34] These magneto-structural studies have shown that the nature and magnitude of the magnetic coupling between the parallel magnetic orbitals depends on the values of the angle at the bridge $\phi$ and the out-of-plane Cu⋯O bond distance ($R_0$).

---

(33) Jotham, R. W.; Kettle, S. F. A. *Inorg. Chim. Acta* **1970**, *4*, 145.

(34) (a) Chiari, B.; Helms, J. H.; Piovesana, O.; Tarantelli, T.; Zanazzi, P. F. *Inorg. Chem.* **1986**, *25*, 2408. (b) Greenway, A. M.; O'Connor, J. C.; Overman, J. W.; Sinn, E. *Inorg. Chem.* **1981**, *20*, 1508. (c) Pasini, A.; Demartin, F.; Piovesana, O.; Chiari, B.; Cinti, A.; Crispu, O. *J. Chem. Soc., Dalton Trans.* **2000**, 3467. (d) Escribá, E.; Server-Carrió, J.; Lezama, L.; Folgado, J. V.; Pizarro, J. L.; Ballesteros, R.; Abarca, B. *J. Chem. Soc., Dalton Trans.* **1997**, 2033.

Values of $\phi = 103.21°$ and $R_0 = 2.371$ Å in **2** allow us to predict a weak antiferromagnetic interaction through this bridge. Looking at the value of $zJ'$ obtained by the fit (ca. $-1.0$ K), the exchange pathway through the double $\mu$-oxo bridge is most likely responsible for this coupling.

## Conclusions

The combined used of Cu(II), malonate, and bpe afforded two malonato-bridged copper(II) complexes of formulas $\{(H_2bpe)[Cu(mal)_2]\}_n \cdot 4nH_2O$ (**1**) (chain compound) and $[Cu_4(mal)_4(bpe)_3]_n \cdot 6nH_2O$ (**2**) (three-dimensional compound) where the bpe molecule is present either as a diprotonated cation that connects uniform $[Cu(mal)_2]^{2-}$ chains through hydrogen bonds (**1**) or as a neutral bis-monodentate ligand that connects malonato-bridged copper(II) layers (**2**). The pH and the copper(II)/malonate molar ratio are the relevant parameters in the synthesis of **1** and **2**. Both compounds exhibit an overall ferromagnetic coupling, the carboxylate-(malonate)-bridging pathway appearing as a sure way to transmit ferromagnetic interactions between copper(II) ions.

**Acknowledgment.** Funding for the work described here is provided by the Ministerio Español de Ciencia y Tecnología through Project BQU2001-3794 and by the Consejería de Educación, Cultura y Deportes del Gobierno Autónomo de Canarias through Project PI2002/175. F.S.D. acknowledges the Gobierno Autónomo de Canarias for a predoctoral fellowship.

**Supporting Information Available:** X-ray crystallographic data in CIF format for **1** and **2**. This material is available free of charge via the Internet at http://pubs.acs.org.

IC034422W